Electronic Research Archive

ERA, 32(1): 405–417.
DOI: 10.3934/era.2024020
Received: 27 September 2023
Revised: 08 December 2023
Accepted: 20 December 2023
Published: 28 December 2023

http://www.aimspress.com/journal/ERA

Research article

Dynamical analysis of spontaneous Ca^{2+} oscillations in astrocytes

Yapeng Zhang[1], Yu Chen[1] and Quanbao Ji[1,2,*]

[1] School of Mathematics and Physics, Guangxi Minzu University, Nanning 530006, China
[2] Center for Applied Mathematics of Guangxi, Guangxi Minzu University, Nanning 530006, China

* **Correspondence:** Email: jqb_2001@163.com.

Abstract: In this work, we focus on a nonlinear dynamical model proposed by Lavrentovich et al. to compute and simulate spontaneous Ca^{2+} oscillations evoked by calcium ion efflux in astrocytes. Selected parameters are chosen, with observation of periodic and chaotic Ca^{2+} oscillations in cytosol. The stability analysis of equilibrium is conducted using the center manifold theorem to investigate the dynamics underlying spontaneous Ca^{2+} oscillations in astrocytes. The results indicate that the Hopf bifurcation represents the dynamical changes in stability of spontaneous Ca^{2+} oscillations. In addition, numerical simulations are performed to further assess the validity of the aforementioned analysis.

Keywords: astrocytes; Hopf bifurcation; center manifold; stability

1. Introduction

Astrocytes have traditionally been auxiliary elements to central nervous system, thereby providing support and nutrients to neurons. Unlike neurons, astrocytes may exert an active role in neuronal firing activities and are extensively employed in research pertaining to diverse neurological disorders [1–5]. Astrocytes do not generate electrical signals themselves but participate in neuronal activity by regulating the release of "glial transmitters", such as glutamate and ATP, through intracellular Ca^{2+} oscillations [6,7]. In the brain, they occupy approximately 50% of the volume and can either be influenced by neurons or exhibit spontaneous Ca^{2+} oscillations [8]. Spontaneous Ca^{2+} oscillations typically encompass the following main processes: (i) channel dynamics; (ii) calcium-induced calcium release; and (iii) negative feedback regulation [9–11]. Many studies have unveiled the correlation between the onset and cessation of Ca^{2+} oscillations within the system [12–15].

Intracellular Ca^{2+} oscillation in astrocytes is frequently triggered by an external stimulus, such

as glutamate. Nevertheless, Aguado et al. [16] observed spontaneous activities in astrocytes, thereby suggesting the existence of potential bidirectional regulation. In fact, astrocytes not only actively participate in neuronal activity and regulate synaptic plasticity, but also contribute to neural repair [17,18]. Therefore, a dynamical analysis of spontaneous Ca^{2+} oscillations could contribute to comprehending the role of astrocytes in neural networks and provide valuable insights into the development of complex brain networks in future. Here, a local Hopf bifurcation of a mathematical model in astrocytes proposed by Lavrentovich et al. [19] is investigated. This model manifests the dynamical behaviors of astrocytes without external stimulation. The objective of this work is to investigate the stability and bifurcation to explore the effects of calcium release rates from the cytosol of astrocytes.

2. Models

The model in [20] considered intracellular Ca^{2+} oscillations triggered by external stimuli, the interplay between calcium induced calcium release and the degradation of inositol triphosphate (IP_3). In [21], the authors proposed a mathematical model that considered experimental data to predict the control and plasticity of intercellular Ca^{2+} waves. Subsequently, Lavrentovich et al. [19] simplified this model and provided an improved framework to evaluate spontaneous Ca^{2+} oscillations in astrocytes. The system is activated by the influx of extracellular Ca^{2+} into the cell and sustained through feedback mechanisms involving intracellular Ca^{2+} in the endoplasmic reticulum (ER) and IP_3. The equations for the temporal evolution of three variables are defined as follows:

$$\begin{cases} dCa_{\text{cyt}}/dt = v_{\text{in}} - k_{\text{out}}Ca_{\text{cyt}} - v_{\text{serca}} + v_{\text{CICR}} + k_{\text{f}}\left(Ca_{\text{er}} - Ca_{\text{cyt}}\right), \\ dCa_{\text{er}}/dt = v_{\text{serca}} - v_{\text{CICR}} - k_{\text{f}}\left(Ca_{\text{er}} - Ca_{\text{cyt}}\right), \\ dIP_3/dt = v_{\text{PLC}} - k_{\text{deg}}IP_3, \end{cases} \tag{1}$$

$$v_{\text{PLC}} = v_{\text{p}}\left(\frac{Ca_{\text{cyt}}^2}{Ca_{\text{cyt}}^2 + k_{\text{p}}^2}\right), v_{\text{serca}} = v_{\text{M2}}\left(\frac{Ca_{\text{cyt}}^2}{Ca_{\text{cyt}}^2 + k_2^2}\right),$$

$$v_{\text{CICR}} = 4v_{\text{M3}}\left(\frac{k_{\text{CaA}}^{\text{n}}Ca_{\text{cyt}}^{\text{n}}}{\left(Ca_{\text{cyt}}^{\text{n}} + k_{\text{CaA}}^{\text{n}}\right)\left(Ca_{\text{cyt}}^{\text{n}} + k_{\text{CaI}}^{\text{n}}\right)}\right) \times \left(\frac{IP_3^{\text{m}}}{IP_3^{\text{m}} + k_{\text{ip3}}^{\text{m}}}\right)\left(Ca_{\text{er}} - Ca_{\text{cyt}}\right).$$

The three variables represent the concentration of Ca^{2+} within the cytosol (Ca_{cyt}), the concentration Ca^{2+} within the ER (Ca_{er}), and the IP_3 concentration (IP_3). The following equations describe the specific meanings of certain parameters, such as the rate of Ca^{2+} pumping into the ER by the reticulum's ATPase (v_{serca}), the rate of Ca^{2+} flux from the ER to the cytosol mediated by the IP_3 receptors (v_{CICR}) and IP_3 production (v_{PLC}). The specific meanings and values of other parameters can be referred to in [19–21].

Table 1. Details of the parameters in Lavrentovich model.

Parameter	Value and units	Description
v_{M2}	15.0 μM/s	maximum Ca^{2+} efflux from the pump
k_{out}	bifurcation parameter	The rate of calcium release from the cytosol
k_{deg}	0.08 s^{-1}	Rate constant of IP_3 degradation
k_{CaA}	0.27 μM	activating affinities
k_{ip3}	0.1 μM	apparent affinity for IP_3
v_{M3}	40.0 s^{-1}	maximum Ca^{2+} flux entering the cytosol
k_2	0.1 μM	threshold constants for pumping
k_{CaI}	0.27 μM	inhibiting affinities
m	2.2	Hill coefficient
n	2.02	Hill coefficient
k_f	0.5 s^{-1}	Leakage flux
v_p	0.05	rate of PLC (phospholipase C) activation
v_{in}	0.05 s^{-1}	Ca^{2+} influx across the plasma membrane
k_p	0.164 μM	Ca^{2+} activation threshold for PLC

3. Stability and bifurcation analysis

k_{out} is selected as the bifurcation parameter. For convenience, we write $\alpha = Ca_{cyt}$, $\beta = Ca_{er}$, $\gamma = IP_3$ and $\theta = k_{out}$. The system dynamics are determined by the following form:

$$\begin{cases} \dot{\alpha} = 0.05 + 0.5\beta - 0.5\alpha - \dfrac{15\alpha^2}{\alpha^2 + 0.01} - \theta\alpha - \dfrac{11.36\alpha^{2.02}\gamma^{2.2}(\alpha - \beta)}{\left(\alpha^{2.02} + 0.07102\right)^2\left(\gamma^{2.2} + 0.00631\right)}, \\ \dot{\beta} = 0.5\alpha - 0.5\beta + \dfrac{15\alpha^2}{\alpha^2 + 0.01} + \dfrac{11.36\alpha^{2.02}\gamma^{2.2}(\alpha - \beta)}{\left(\alpha^{2.02} + 0.07102\right)^2\left(\gamma^{2.2} + 0.00631\right)}, \\ \dot{\gamma} = \dfrac{0.05\alpha^2}{\alpha^2 + 0.0269} - 0.08\gamma. \end{cases} \tag{2}$$

The equilibrium points satisfy the equations on the left side of system (2) when they equal zero. Subsequently, by calculating

$$\frac{0.05\alpha^2}{\alpha^2 + 0.0269} - 0.08\gamma = 0,$$

we can obtain

$$\gamma = \frac{0.05\alpha^2}{0.08(\alpha^2 + 0.0269)}.$$

Then,

$$0.5\alpha - 0.5\beta + \frac{15\alpha^2}{\alpha^2 + 0.01} + \frac{11.36\alpha^{2.02}\gamma^{2.2}(\alpha - \beta)}{\left(\alpha^{2.02} + 0.07102\right)^2\left(\gamma^{2.2} + 0.00631\right)} = 0$$

can be obtained by

$$\beta = \frac{0.5\alpha + \dfrac{15\alpha^2}{\alpha^2+0.01} + \dfrac{11.36\alpha^{3.02}\sigma_1}{(\sigma_1+0.00631)\left(\alpha^{2.02}+0.07102\right)^2}}{\dfrac{11.36\alpha^{2.02}\sigma_1}{(\sigma_1+0.00631)\left(\alpha^{2.02}+0.07102\right)^2}+0.5},$$

$$\sigma_1 = \left(\frac{5\alpha^2}{8\alpha^2+0.2152}\right)^{2.2}.$$

Subsequently, by substituting β and γ into the equation

$$0.05+0.5\beta-0.5\alpha-\frac{15\alpha^2}{\alpha^2+0.01}-\theta\alpha-\frac{11.36\alpha^{2.02}\gamma^{2.2}(\alpha-\beta)}{\left(\alpha^{2.02}+0.07102\right)^2\left(\gamma^{2.2}+0.00631\right)}=0,$$

we have the following:

$$\begin{cases} f(\alpha,\theta)=0.05+0.5\beta-0.5\alpha-\dfrac{15\alpha^2}{\alpha^2+0.01}-\theta\alpha-\dfrac{11.36\alpha^{2.02}\gamma^{2.2}(\alpha-\beta)}{\left(\alpha^{2.02}+0.07102\right)^2\left(\gamma^{2.2}+0.00631\right)}=0 \\ \beta=\dfrac{0.5\alpha+\dfrac{15\alpha^2}{\alpha^2+0.01}+\dfrac{11.3625\alpha^{3.02}\sigma_1}{(\sigma_1+0.0063)\left(\alpha^{2.02}+0.071\right)^2}}{\dfrac{11.3625\alpha^{2.02}\sigma_1}{(\sigma_1+0.0063)\left(\alpha^{2.02}+0.071\right)^2}+0.5} \\ \gamma=\dfrac{0.05\alpha^2}{0.08(\alpha^2+0.0269)}. \end{cases} \tag{3}$$

Assuming that the equilibrium points are denoted as $\alpha_0, \beta_0, \gamma_0$, we have the following equations through the substitution $j_1 = j - j_0$ ($j = \alpha, \beta, \gamma$):

$$\begin{cases} \dot{\alpha}_1 = 0.05+0.5(\beta_1+\beta_0)-0.5(\alpha_1+\alpha_0)-\dfrac{15(\alpha_1+\alpha_0)^2}{(\alpha_1+\alpha_0)^2+0.01}-\theta(\alpha_1+\alpha_0) \\ -\dfrac{11.36(\alpha_1+\alpha_0)^{2.02}\gamma^{2.2}\left((\alpha_1+\alpha_0)-(\beta_1+\beta_0)\right)}{\left((\alpha_1+\alpha_0)^{2.02}+0.07102\right)^2\left((\gamma_1+\gamma_0)^{2.2}+0.00631\right)}, \\ \dot{\beta}_1 = 0.5(\alpha_1+\alpha_0)-0.5(\beta_1+\beta_0)+\dfrac{15(\alpha_1+\alpha_0)^2}{(\alpha_1+\alpha_0)^2+0.01} \\ +\dfrac{11.36(\alpha_1+\alpha_0)^{2.02}(\gamma_1+\gamma_0)^{2.2}\left((\alpha_1+\alpha_0)-(\beta_1+\beta_0)\right)}{\left((\alpha_1+\alpha_0)^{2.02}+0.07102\right)^2\left((\gamma_1+\gamma_0)^{2.2}+0.00631\right)}, \\ \dot{\gamma}_1 = \dfrac{0.05(\alpha_1+\alpha_0)^2}{(\alpha_1+\alpha_0)^2+0.0269}-0.08(\gamma_1+\gamma_0). \end{cases} \tag{4}$$

Systems (2) and (4) could exhibit identical characteristics with mutual equilibrium points (0, 0, 0). Therefore, we can readily compute the Jacobian matrix of the system as follows:

$$J = \begin{pmatrix} i_{11} & i_{12} & i_{13} \\ i_{21} & i_{22} & i_{23} \\ i_{31} & i_{32} & i_{33} \end{pmatrix}$$

where

$$\begin{pmatrix} \sigma_1 - \theta - \dfrac{30\alpha}{\alpha^2 + 0.01} - \sigma_2 - \sigma_6 + \sigma_5 - 0.5 & \sigma_2 + 0.5 & \sigma_3 - \sigma_4 \\ \dfrac{30\alpha}{\alpha^2 + 0.01} - \sigma_1 + \sigma_2 + \sigma_6 - \sigma_5 + 0.5 & -\sigma_2 - 0.5 & \sigma_4 - \sigma_3 \\ \dfrac{0.1\alpha}{\alpha^2 + 0.026896} - \dfrac{0.1\alpha^3}{\left(\alpha^2 + 0.026896\right)^2} & 0 & -0.08 \end{pmatrix}$$

$$\sigma_1 = \frac{30\alpha^3}{\left(\alpha^2 + 0.01\right)^2};\ \sigma_2 = \frac{11.363\alpha^{2.02}\gamma^{2.2}}{\sigma_7}\ ;\ \sigma_3 = \frac{24.998\alpha^{2.02}\gamma^{3.4}\left(\alpha - \beta\right)}{\left(\alpha^{2.02} + 0.071016\right)^2 {\sigma_8}^2};$$

$$\sigma_4 = \frac{24.998\alpha^{2.02}\gamma^{1.2}\left(\alpha - \beta\right)}{\sigma_7};\ \sigma_5 = \frac{45.905\alpha^{3.04}\gamma^{2.2}\left(\alpha - \beta\right)}{\left(\alpha^{2.02} + 0.071016\right)^3 \sigma_8};$$

$$\sigma_6 = \frac{22.952\alpha^{1.02}\gamma^{2.2}\left(\alpha - \beta\right)}{\sigma_7};\ \sigma_7 = \left(\alpha^{2.02} + 0.071016\right)^2 \sigma_8;$$

$$\sigma_8 = \gamma^{2.2} + 0.0063096.$$

The resulting characteristic equation can be easily obtained using the following:

$$\lambda^3 + Q_3\lambda^2 + Q_2\lambda + Q_1 = 0,$$

where

$$\begin{aligned} Q_1 &= -(i_{11} + i_{22} + i_{33}), \\ Q_2 &= i_{11}i_{22} + i_{11}i_{33} + i_{22}i_{33} - i_{13}i_{31} - i_{12}i_{21} - i_{32}i_{23}, \\ Q_3 &= i_{31}i_{13}i_{22} + i_{12}i_{21}i_{33} + i_{32}i_{23}i_{11} - i_{11}i_{22}i_{33} - i_{12}i_{23}i_{31} - i_{13}i_{21}i_{32}. \end{aligned}$$

The characteristic polynomial can be obtained and the Hurwitz matrix with Q_l (l = 1, 2, 3) coefficients is as follows:

$$H_1 = \left(Q_1\right), H_2 = \begin{pmatrix} Q_1 & 1 \\ Q_3 & Q_2 \end{pmatrix}, H_3 = \begin{pmatrix} Q_1 & 1 & 0 \\ Q_3 & Q_2 & 1 \\ 0 & 0 & Q_3 \end{pmatrix}.$$

The stability of the system can be determined by calculating the sign of H_l (l = 1, 2, 3). The dynamical behaviors of the system (4) can be obtained as the parameter k_{out} varies with use of the Routh-Hurwitz criteria [12].

When

1) θ < 0.421, there is a stable node;
2) θ = 0.421, there is a Hopf bifurcation point O_1 = (0.1183, 0.5907, 0.2146);
3) 0.421 < θ < 1.267, there exists an equilibrium;
4) θ = 1.267, there is a Hopf bifurcation point O_2 = (0.0345, 2.6574, 0.0246);
5) 1.267 < θ ≤ 1.284, there exists an equilibrium; and
6) θ > 1.284, there is a stable node.

Given $j_1 = j - j_0$ ($j = \alpha, \beta, \gamma, \theta$), the equilibrium of system (4) is (α_0, β_0, γ_0). We introduce a new parameter θ_1 for $\mathrm{d}\theta_1/dt = 0$.

$$\begin{cases} \dot{\alpha}_1 = 0.05 + 0.5(\beta_1 + \beta_0) - 0.5(\alpha_1 + \alpha_0) - \dfrac{15.0(\alpha_1 + \alpha_0)^2}{(\alpha_1 + \alpha_0)^2 + 0.01} - (\theta_1 + \theta_0)(\alpha_1 + \alpha_0) \\ -\dfrac{11.36(\alpha_1 + \alpha_0)^{2.02}\gamma^{2.2}((\alpha_1 + \alpha_0) - (\beta_1 + \beta_0))}{\left((\alpha_1 + \alpha_0)^{2.02} + 0.07102\right)^2\left((\gamma_1 + \gamma_0)^{2.2} + 0.00631\right)}, \\ \dot{\beta}_1 = 0.5(\alpha_1 + \alpha_0) - 0.5(\beta_1 + \beta_0) + \dfrac{15(\alpha_1 + \alpha_0)^2}{(\alpha_1 + \alpha_0)^2 + 0.01} \\ +\dfrac{11.36(\alpha_1 + \alpha_0)^{2.02}(\gamma_1 + \gamma_0)^{2.2}((\alpha_1 + \alpha_0) - (\beta_1 + \beta_0))}{\left((\alpha_1 + \alpha_0)^{2.02} + 0.07102\right)^2\left((\gamma_1 + \gamma_0)^{2.2} + 0.00631\right)}, \\ \dot{\gamma}_1 = \dfrac{0.05(\alpha_1 + \alpha_0)^2}{(\alpha_1 + \alpha_0)^2 + 0.0269} - 0.08(\gamma_1 + \gamma_0), \\ \dot{\theta}_1 = 0. \end{cases} \tag{5}$$

Systems (2) and (5) have the same dynamics with mutual equilibrium points O (α_1, β_1, γ_1, θ_1) = (0, 0, 0, 0). For θ_0 = 0.421, we calculate the eigenvalues at the equilibrium point: ξ_1 = –0.1200, ξ_2 = 2.2814i, ξ_3 = –2.2814i and ξ_4 = 0. The eigenvectors conform to the ensuing matrix:

$$\begin{pmatrix} -0.1825 & -0.6869 - 0.1263i & -0.6869 + 0.1263i & -0.1920 \\ -0.4592 & 0.7134 & 0.7134 & 0.5352 \\ 0.8694 & -0.0139 + 0.0565i & -0.0139 - 0.0565i & -0.4566 \\ 0 & 0 & 0 & 0.6843 \end{pmatrix}.$$

Suppose

$$\begin{pmatrix} \alpha_1 \\ \beta_1 \\ \gamma_1 \\ \theta_1 \end{pmatrix} = U \begin{pmatrix} \mathrm{x} \\ y \\ z \\ s \end{pmatrix}, \quad U = \begin{pmatrix} -0.1825 & -0.6869 & 0.1263 & -0.1920 \\ -0.4592 & 0.7134 & 0 & 0.5352 \\ 0.8694 & -0.0139 & -0.0565 & -0.4566 \\ 0 & 0 & 0 & 0.6843 \end{pmatrix}.$$

System (5) can be replaced by

$$\begin{pmatrix} \dot{x} \\ \dot{y} \\ \dot{z} \\ \dot{s} \end{pmatrix} = \begin{pmatrix} -0.1200 & 0 & 0 & 0 \\ 0 & 0 & -2.2814 & 0 \\ 0 & 2.2814 & 0 & 0 \\ 0 & 0 & 0 & 0 \end{pmatrix} \begin{pmatrix} x \\ y \\ z \\ s \end{pmatrix} + \begin{pmatrix} g_1 \\ g_2 \\ g_3 \\ g_4 \end{pmatrix}, \tag{6}$$

and

$$\begin{pmatrix}\dot{\alpha}_1\\ \dot{\beta}_1\\ \dot{\gamma}_1\\ \dot{\theta}_1\end{pmatrix}=U\begin{pmatrix}\dot{x}\\ \dot{y}\\ \dot{z}\\ \dot{s}\end{pmatrix}\Rightarrow\begin{pmatrix}\dot{x}\\ \dot{y}\\ \dot{z}\\ \dot{s}\end{pmatrix}=U^{-1}\begin{pmatrix}\dot{\alpha}_1\\ \dot{\beta}_1\\ \dot{\gamma}_1\\ \dot{\theta}_1\end{pmatrix}=U^{-1}\begin{pmatrix}f_1\\ f_2\\ f_3\\ 0\end{pmatrix}$$

$$\begin{pmatrix}g_1\\ g_2\\ g_3\\ g_4\end{pmatrix}=U^{-1}\begin{pmatrix}f_1\\ f_2\\ f_3\\ 0\end{pmatrix}-\begin{pmatrix}-0.1200 & 0 & 0 & 0\\ 0 & 0 & -2.2814 & 0\\ 0 & 2.2814 & 0 & 0\\ 0 & 0 & 0 & 0\end{pmatrix}\begin{pmatrix}x\\ y\\ z\\ s\end{pmatrix},$$

where

$$\begin{aligned}
&g_1=-0.7699f_1-0.7749f_2+1.7211f_3-0.12x,\\
&g_2=0.4956f_1+1.9005f_2+1.1078\mathrm{f}_3-2.2814z,\\
&g_3=11.7255f_1+11.4558f_2+8.5121f_3+2.2814y,\\
&g_4=0,\\
&f_1=0.3636s-0.1383x+0.7001y-0.06315z-\sigma_2+\left(0.6843s+0.4217\right)\sigma_5+\sigma_1+0.2862,\\
&f_2=0.1383x-0.3636s-0.7001y+0.06315z+\sigma_2-\sigma_1-0.2362,\\
&f_3=0.03653s-0.06955x+0.001112y+0.00452z+\frac{0.05{\sigma_5}^2}{{\sigma_5}^2+0.0269}-0.01717,\\
&f_4=0,\\
&\sigma_1=\frac{11.36\left(0.7272s-0.2767x+1.4y-0.1263z+0.4724\right)\sigma_3\sigma_4}{\left(\sigma_4+0.00631\right)\left(\sigma_3+0.07102\right)^2},\\
&\sigma_2=\frac{15.0{\sigma_5}^2}{{\sigma_5}^2+0.01},\\
&\sigma_3=\left(0.1263z-0.1825x-0.6869y-0.192s+0.1183\right)^{2.02},\\
&\sigma_4=\left(0.8694x-0.4566s-0.0139y-0.0565z+0.2146\right)^{2.2},\\
&\sigma_5=0.192s+0.1825x+0.6869y-0.1263z-0.1183.
\end{aligned}$$

System (5) has a center manifold with the following form:

$$W_{\mathrm{loc}}^{\mathrm{c}}\left(O_1\right)=\left\{(\mathrm{x},\mathrm{y},z,s)\in R^4\mid x=h^*(y,z,s),h^*(0,0,0)=0,Dh^*(0,0,0)=0\right\}.$$

Substituting the equation into (6) yields the following equations:

$$\begin{pmatrix}\dot{h}^*(y,z,s)\\ \dot{y}\\ \dot{z}\\ \dot{s}\end{pmatrix}=\begin{pmatrix}-0.1200 & 0 & 0 & 0\\ 0 & 0 & -2.2814 & 0\\ 0 & 2.2814 & 0 & 0\\ 0 & 0 & 0 & 0\end{pmatrix}\begin{pmatrix}h^*(y,z,s)\\ y\\ z\\ s\end{pmatrix}+\begin{pmatrix}g_1\\ g_2\\ g_3\\ g_4\end{pmatrix}.$$

Let $h\,(y, z, s) = ay^2 + bz^2 + cs^2 + dyz + eys + fzs + \ldots$; we have the following:

$$N(h) = Dh \cdot \begin{bmatrix} \dot{y} \\ \dot{z} \\ \dot{s} \end{bmatrix} + 0.12h - g_1 \equiv 0, \tag{7}$$

where a = –0.7494, b = –0.7334, c = –2.1352, d = –0.0752, e = –0.0506, f = –0.2795. The system is described as follows:

$$\begin{pmatrix} \dot{y} \\ \dot{z} \end{pmatrix} = \begin{pmatrix} 0 & -2.2814 \\ 2.2814 & 0 \end{pmatrix} \begin{pmatrix} y \\ z \end{pmatrix} + \begin{pmatrix} f(y,z) \\ g(y,z) \end{pmatrix}, \tag{8}$$

where

$$f(y,z) = 2.375z - 0.9824y - 0.4704s - 0.005937sy - 0.0328sz - 0.008823yz \cdots,$$
$$g(y,z) = 0.02144z - 2.083y + 0.409s + 0.03185sy + 0.1759sz + 0.04733yz + 1.344s^2 + \cdots.$$

Hence, it is easy to obtain the following:

$$\begin{aligned} a = {} & \frac{1}{16}[f^1_{yyy} + f^1_{yzz} + f^2_{yyz} + f^2_{zzz}]\Big|_{(0,0)} + \frac{1}{16 \times 2.2814}[f^1_{yz}(f^1_{yy} + f^1_{zz}) \\ & - f^2_{yz}(f^2_{yy} + f^2_{zz}) - f^1_{yy}f^2_{yy} + f^1_{zz}f^2_{zz})]\Big|_{(y=0,z=0,s=0)} = -270.7099 < 0, \\ d = {} & \frac{d(\mathrm{Re}(\xi(s)))}{ds}\Big|_{(y=0,z=0,s=0)} = -0.3697 < 0. \end{aligned} \tag{9}$$

Based on the aforementioned computation, we derive the following conclusions.

Conclusion 1: A subcritical Hopf bifurcation is observed as the parameter θ traverses the critical value of θ_0 = 0.421. Below this threshold ($\theta < \theta_0$), the equilibrium O_1 is always locally stable. For $\theta > \theta_0$, the equilibrium O_1 turns to be unstable. and the system (2) begins to oscillate.

For θ_0 = 1.267, the eigenvalues at the equilibrium point can be computed as follows: ξ_1 = –69.3501, ξ_2 = 0.0157i, ξ_3 = –0.0157i and ξ_4 = 0.

$$\begin{pmatrix} \dot{y} \\ \dot{z} \end{pmatrix} = \begin{pmatrix} 0 & -0.0157 \\ 0.0157 & 0 \end{pmatrix} \begin{pmatrix} y \\ z \end{pmatrix} + \begin{pmatrix} f(y,z) \\ g(y,z) \end{pmatrix}, \tag{10}$$

where

$$f(y,z) = 0.006927s - 0.008238y + 0.01683z + 0.0006307sy + 0.0005685sz - 0.0007773yz + \cdots,$$
$$g(y,z) = 0.02448s - 0.05694y - 0.08124z - 0.001969sy - 0.001775sz + 0.002427yz + \cdots.$$

Similar to the previous computations, we have a = –0.12945 < 0 and d = –0.0113 < 0.

Conclusion 2: system (2) undergoes a supcritical Hopf bifurcation at θ_0 = 1.267. When $\theta < \theta_0$, the equilibrium O_2 turns to be unstable.

4. Numerical simulations

Next, we present the bifurcation diagrams by varying the values of parameter k_{out}, as illustrated in Figure 1a,b. As k_{out} varies from 0.2 to 1.5, the system undergoes bifurcations around 0.421 and 1.267. Figure 1a illustrates the bifurcation in terms of both the period and the amplitude. When the parameter value is between 0.42 and 0.49, the model exhibits a simple oscillation with a consistent amplitude. As k_{out} is further increased, the model displays complex Ca^{2+} oscillations with varying amplitudes and periods. The period gradually decreases near 1.28. In Figure 1b, the continuous line represents the equilibrium state. HB1 and HB2 correspond to two bifurcation points. Figure 1c displays the interspike interval (ISI) bifurcation. As the parameter increases, the value of ISI becomes larger, thereby indicating a decrease in frequency. Figure 1d depicts the corresponding Lyapunov exponent diagram.

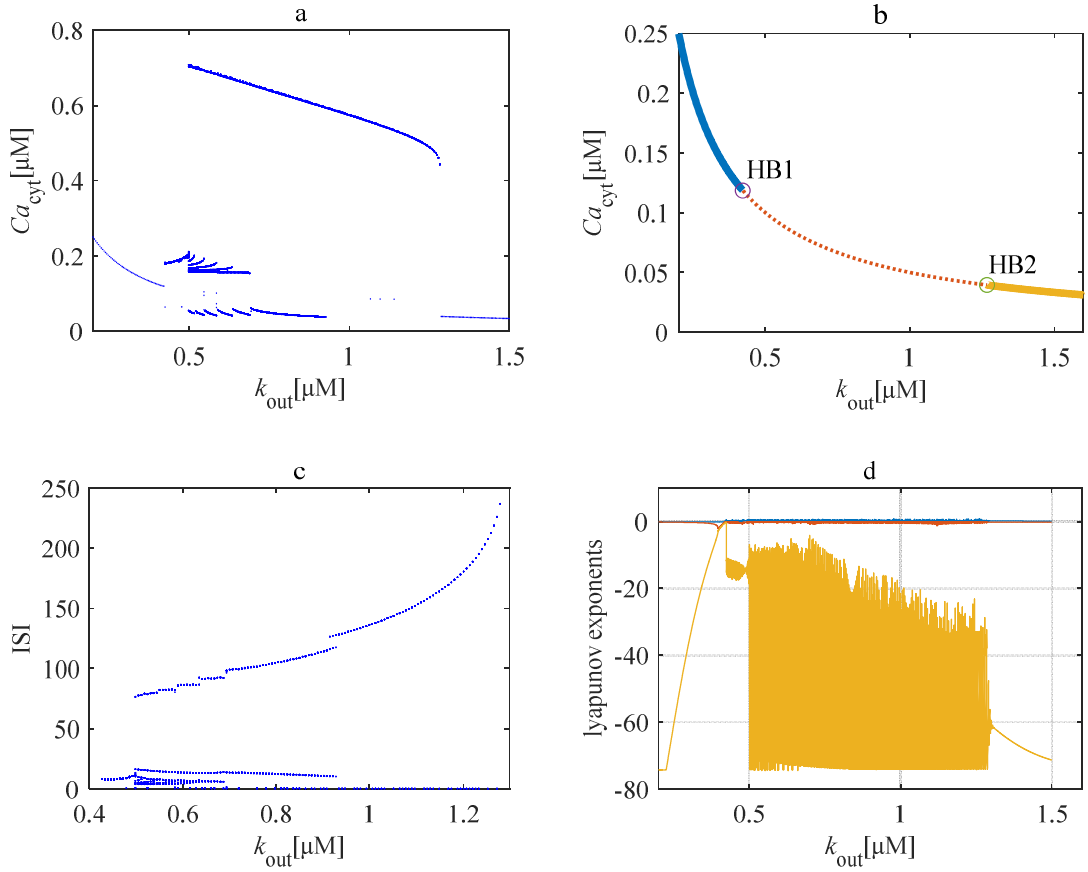

Figure 1. (a) The interspike interval bifurcation diagram with k_{out}. (b) Bifurcation diagram in (k_{out}, Ca_{cyt}) plane, HB represents Hopf bifurcation points. (c) The interspike interval bifurcation diagram with k_{out}. (d) Lyapunov exponent with parameter k_{out}.

In Figure 2, we present the time course for different values of the parameter k_{out}. The left column displays the time series for different parameter values (Figure 2a1–f1), the middle column shows the corresponding phase portraits (Figure 2a2–f2) and the right column illustrates the variations in power and frequency for the corresponding time series (Figure 2a3–f3). For example,

Figure 2a1 represents the time course of Ca^{2+} evolution for k_{out} = 1.2. To eliminate the initial value interference, the time evolution for the first 200 s is excluded, thus allowing only one peak to appear in the graph. In Figure 2a2, a periodic orbit is evident. Figure 2a3 illustrates its frequency variation.

In Figure 2b1, we present spontaneous bursting Ca^{2+} oscillations for k_{out} = 0.7. In Figure 2c1–e1, an increasing number of small spikes become apparent. The corresponding phase portrait diagrams are illustrated in Figure 2b2–e2. Figure 2f1 corresponds to the case with k_{out} = 0.4966 in the bifurcation diagram. The time series illustrates the phenomenon of bursting chaos. For a clearer representation, we have zoomed in on the time range of 10,000 s. The upper right corner depicts a schematic of the local magnification.

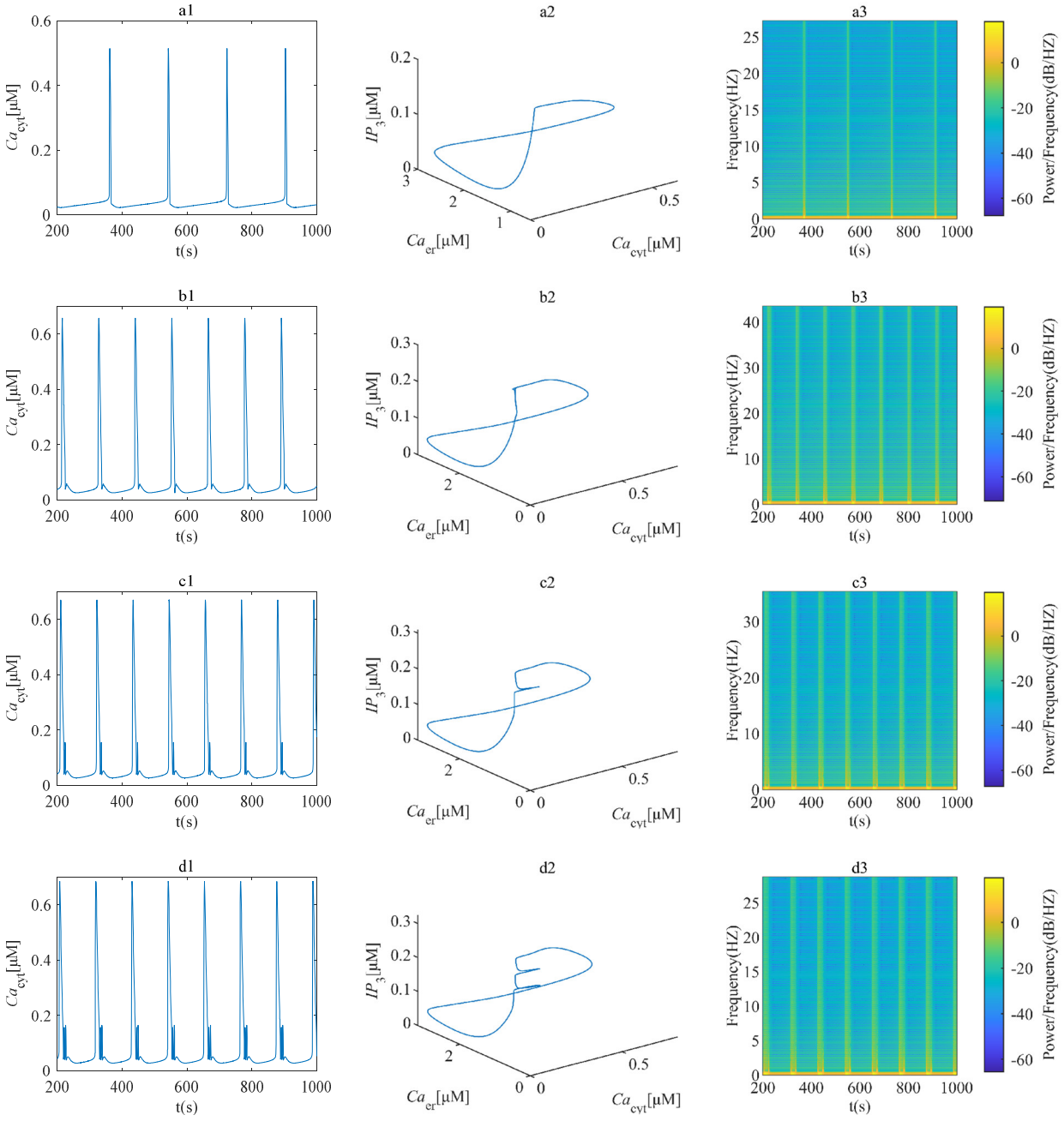

Continued on next page

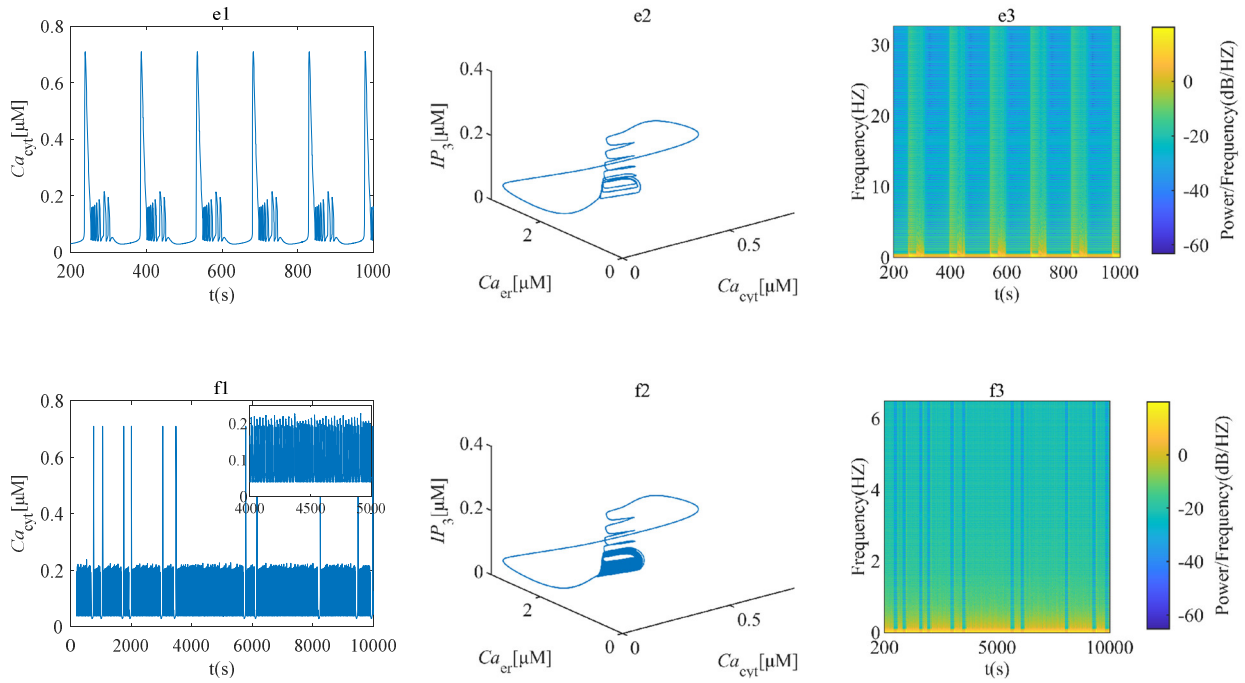

Figure 2. Illustrations for spontaneous Ca^{2+} oscillations. The left side displays the time series for Ca_{cyt}. The middle graphs are the associated phase portraits. The right panels display the variations in power and frequency. Different values of k_{out} in each figure are: (a1–a3) k_{out} = 1.2 s^{-1}; (b1–b3) k_{out} = 0.7 s^{-1}; (c1–c3) k_{out} = 0.65 s^{-1}; (d1–d3) k_{out} = 0.6 s^{-1}; (e1–e3) k_{out} = 0.5 s^{-1} and (f1–f3) k_{out} = 0.4966 s^{-1}.

5. Discussion

In this paper, we investigated the stability and bifurcation of spontaneous Ca^{2+} oscillations in astrocytes using a well-established mathematical model which measures the rate of calcium release from the cytosol as a controlling parameter. Within a specific range, we identified two Hopf bifurcation points. The stability analysis revealed their close association with spontaneous Ca^{2+} oscillations. To validate the theoretical predictions, numerical simulations were conducted to demonstrate the consistency with computations. When the parameters were varied, the stability of the system exhibited diverse dynamic behaviors.

We analyzed the spontaneous Ca^{2+} oscillations evoked by calcium ion efflux in astrocytes in the same model as compared with previous studies [12,19], and obtained more complex dynamical behaviors. For instance, as the rate of calcium release from the cytosol decreased, this model exhibited the gradual emergence of multiple peaks simultaneously, accompanied by an increasing number of smaller peaks, before culminating in irregular chaotic states. Time-frequency diagrams were presented to show more intuitive depictions of frequency changes. The complexity arose from bidirectional communication between neurons and astrocytes and significantly increased the richness of their dynamical behavior. Future research is needed to examine the potential dynamical mechanisms for bidirectional communication in detail.

Use of AI tools declaration

The authors declare they have not used Artificial Intelligence (AI) tools in the creation of this article.

Acknowledgments

This work was supported by the National Natural Science Foundation of China (No. 12062004), the Natural Science Foundation of Guangxi Minzu University (No. 2022KJQD01), the Guangxi Natural Science Foundation (2020GXNSFAA297240) and Guangxi Science and Technology Program (Grant No. AD23023001) and Xiangsi Lake Young Scholars Innovation Team of Guangxi Minzu University (No. 2021RSCXSHQN05).

Conflict of Interests

The authors declare there is no conflict of interest.

References

1. J. L. Stobart, K. D. Ferrari, M. J. Barrett, Long-term in vivo calcium imaging of astrocytes reveals distinct cellular compartment responses to sensory stimulation, *Cereb. Cortex*, **28** (2018), 184–198. https://doi.org/10.1093/cercor/bhw366
2. G. Perea, A. Araque, Astrocytes potentiate transmitter release at single hippocampal synapses, *Science*, **317** (2007), 1083–1086. https://doi.org/10.1126/science.1144640
3. A. Covelo, A. Araque, Lateral regulation of synaptic transmission by astrocytes, *Neuroscience*, **323** (2016), 62–66. https://doi.org/10.1016/j.neuroscience.2015.02.036
4. Z. Cao, L. Du, H. Zhang, L. Qiu, L. Yan, Z. Deng, Firing activities and magnetic stimulation effects in a Cortico-basal ganglia-thalamus neural network, *Electron. Res. Arch.*, **30** (2022), 2054–2074. https://doi.org/10.3934/era.2022104
5. Z. Wang, Y. Yang, L. Duan, Dynamic mechanism of epileptic seizures induced by excitatory pyramidal neuronal population, *Electron. Res. Arch.*, **31** (2023), 4427–4442. https://doi.org/10.3934/era.2023226
6. G. Wallach, J. Lallouette, N. Herzog, M. De Pittà, E. B. Jacob, H. Berry, et al., Glutamate mediated astrocytic filtering of neuronal activity, *PLoS Comput. Biol.*, **10** (2014), e1003964. https://doi.org/10.1371/journal.pcbi.1003964
7. A. Volterra, J. Meldolesi, Astrocytes, from brain glue to communication elements: the revolution continues, *Nat. Rev. Neurosci.*, **6** (2005), 626–640. https://doi.org/10.1038/nrn1722
8. E. V. Pankratova, M. S. Sinitsina, S. Gordleeva, V. B. Kazantsev, Bistability and chaos emergence in spontaneous dynamics of astrocytic calcium concentration, *Mathematics*, **10** (2022), 1337. https://doi.org/10.3390/math10081337
9. K. A. Woll, F. V. Petegem, Calcium-release channels: structure and function of IP_3 receptors and ryanodine receptors, *Physiol. Rev.*, **102** (2022), 209–268. https://doi.org/10.1152/physrev.00033.2020

10. S. Zeng, B. Li, S. Zeng, S. Chen, Simulation of spontaneous Ca^{2+} oscillations in astrocytes mediated by voltage-gated calcium channels, *Biophys. J.*, **97** (2009), 2429–2437. https://doi.org/10.1016/j.bpj.2009.08.030
11. Y. Wang, A. K. Fu, N. Y. Ip, Instructive roles of astrocytes in hippocampal synaptic plasticity: neuronal activity-dependent regulatory mechanisms, *FEBS J.*, **289** (2022), 2202–2218. https://doi.org/10.1111/febs.15878
12. H. Zuo, M. Ye, Bifurcation and numerical simulations of Ca^{2+} oscillatory behavior in astrocytes, *Front. Phys.*, **8** (2020), 258. https://doi.org/10.3389/fphy.2020.00258
13. Q. Ji, Y. Zhou, Z. Yang, X. Meng, Evaluation of bifurcation phenomena in a modified Shen–Larter model for intracellular Ca^{2+} bursting oscillations, *Nonlinear Dyn.*, **84** (2016), 1281–1288. https://doi.org/10.1007/s11071-015-2566-3
14. X. Qie, Q. Ji, Computational analysis and bifurcation of regular and chaotic Ca^{2+} oscillations, *Mathematics*, **9** (2021), 3324. https://doi.org/10.3390/math9243324
15. L. Li, Z. Zhao, Inhibitory autapse with time delay induces mixed-mode oscillations related to unstable dynamical behaviors near subcritical Hopf bifurcation, *Electron. Res. Arch.*, **30** (2022), 1898–1917. https://doi.org/10.3934/era.2022096
16. F. Aguado, J. F. Espinosa-Parrilla, M. A. Carmona, E. Soriano, Neuronal activity regulates correlated network properties of spontaneous calcium transients in astrocytes in situ, *J. Neurosci.*, **22** (2002), 9430–9444. https://doi.org/10.1523/JNEUROSCI.22-21-09430.2002
17. A. J. Barker, E. M. Ullian, New roles for astrocytes in developing synaptic circuits, *Commun. Integr. Biol.*, **1** (2008), 207–211. https://doi.org/10.4161/cib.1.2.7284
18. R. A. Chiareli, G. A. Carvalho, B. L. Marques, L. S. Mota, O. C. Oliveira-Lima, R. M. Gomes, et al., The role of astrocytes in the neurorepair process, *Front. Cell Dev. Biol.*, **9** (2021), 665795. https://doi.org/10.3389/fcell.2021.665795
19. M. Lavrentovich, S. Hemkin, A mathematical model of spontaneous calcium (II) oscillations in astrocytes, *J. Theor. Biol.*, **251** (2008), 553–560. https://doi.org/10.1016/j.jtbi.2007.12.011
20. G. Houart, G. Dupont, A. Goldbeter, Bursting, chaos and birhythmicity originating from self-modulation of the inositol 1, 4, 5-trisphosphate signal in a model for intracellular Ca^{2+} oscillations, *Bull. Math. Biol.*, **61** (1999), 507–530. https://doi.org/10.1006/bulm.1999.0095
21. T. Höfer, L. Venance, C. Giaume, Control and plasticity of intercellular calcium waves in astrocytes: a modeling approach, *J. Neurosci.*, **22** (2002), 4850–4859. https://doi.org/10.1523/JNEUROSCI.22-12-04850.2002

AIMS Press